Cancer Letters 459 (2019) 268–276

Contents lists available at ScienceDirect

Cancer Letters

journal homepage: www.elsevier.com/locate/canlet

Original Articles

# The anthelmintic flubendazole blocks human melanoma growth and metastasis and suppresses programmed cell death protein-1 and myeloid-derived suppressor cell accumulation

Yue Li[a], Grishma Acharya[b], Mina Elahy[a], Hong Xin[b], Levon M. Khachigian[a,*]

[a] Vascular Biology and Translational Research, School of Medical Sciences, UNSW Medicine, University of New South Wales, Sydney, NSW, 2052, Australia
[b] Explora BioLabs, Flintkote Avenue, San Diego, CA, 92121, USA

ARTICLE INFO

*Keywords:*
Flubendazole
Melanoma
Programmed cell death protein-1
Myeloid-derived suppressor cells

ABSTRACT

The incidence of melanoma is increasing faster than any other cancer. In recent years, treatment of melanoma and a range of other deadly cancers has involved immunotherapy with programmed cell death protein-1 (PD-1)/PD-1 ligand (PD-L1) checkpoint blockade which has improved survival. However, many patients do not respond or have partial response, survival benefit is in the order of months and all available PD-1/PD-L1 strategies are antibodies requiring intravenous infusion. There are no clinically approved small molecule pharmacologic inhibitors of the PD-1/PD-L1 system. The benzimidazole derivative flubendazole is a widely used anthelmintic available over the counter in Europe. Here we demonstrate the ability of flubendazole to inhibit human melanoma growth and spread in mice. Flubendazole's ability to block tumor growth and spread was comparable to paclitaxel. Anti-tumor effects were observed when flubendazole was delivered systemically not locally. Flubendazole inhibited CD31/PECAM-1 staining indicating suppression of tumor angiogenesis. Most surprisingly, flubendazole inhibited PD-1 levels within the tumors, but not PD-L1. Western blotting and flow cytometry revealed that flubendazole inhibits PD-1 expression in cultured melanoma cells. Flubendazole also reduced myeloid-derived suppressor cell (MDSC) levels in tumor tissue. Further we found that flubendazole inhibited active (phospho-Tyr$^{705}$) signal transducer and activator of transcription (STAT3), an upstream regulator of PD-1 expression. These findings uncover that flubendazole is a novel small molecule inhibitor of not only melanoma growth and spread but also of PD-1 and MDSC.

## 1. Introduction

Melanoma is the deadliest form of skin cancer and its incidence is increasing faster than any other cancer [1]. Historically, treatment for melanoma has been surgery, radiotherapy and chemotherapy [2]. This has changed dramatically in recent years with the introduction of BRAF and MEK inhibitors, and improvements in immunotherapy with programmed cell death protein-1 (PD-1) and CTLA4 inhibitors, first as monotherapy and now in combination. Patient outcomes have improved as a consequence, with median overall survival of patients with advanced-stage melanoma increasing from approximately 9 months prior to 2011 to at least 2 years [3].

PD-1 and programmed cell death 1 ligand 1 (PD-L1) are immune system regulators that play a role in dampening the immune response to cancer cells [4]. PD-1 is a 288 amino acid co-inhibitory receptor from the CD28 family expressed by T cells, B cells, natural killer (NK) cells and some myeloid cell populations [5]. PD-1 typically binds to tumor surface PD-L1 and prevents tumor cell destruction (cytolysis) by immune cells. Interestingly, PD-1 is also expressed by tumor cells [6] including a range of human melanoma cell lines. Kleffel et al. found that PD-1 is expressed by A375, C8161, G3361, FEMX, LOX, MeWo, SK-MEL-28 and UACC-257 cells, with only minor cell fractions positive for PD-1 [7]. PD-L1 is expressed by tumor cells, and by hematopoietic and non-hematopoietic cells [8].

PD-1 inhibitors have changed the cancer treatment paradigm in melanoma and many other deadly cancers including head and neck cancer, non-small cell lung cancer, urothelial cancer, renal cell carcinoma, Hodgkin lymphoma, gastric cancer, colorectal cancer, hepatocellular carcinoma and Merkel cell carcinoma [9]. Hence patient response to immune checkpoint inhibitor therapy does not appear to be restricted to a specific tumor type [10].

However with PD-1/PD-L1 immunotherapy significant challenges

* Corresponding author.
*E-mail address:* L.Khachigian@unsw.edu.au (L.M. Khachigian).

https://doi.org/10.1016/j.canlet.2019.05.026
Received 14 November 2018; Received in revised form 28 March 2019; Accepted 19 May 2019
0304-3835/ 

remain and new ones have arisen. For example, the objective response rate (ORR) of nivolumab monotherapy in previously untreated patients with unresectable stage III or IV melanoma is approximately 40% [11]. Moreover, PD-1/PD-L1 immunotherapy has only modest benefit in other cancer types. For example, KEYNOTE-012 evaluating pembrolizumab efficacy and safety in head and neck cancer patients showed that the ORR was 18% and overall survival (OS) at 12 months was 38% [12]. In KEYNOTE-055 the ORR was 16% with a median duration of response of 8 months [13]. In CHECKMATE-141, OS was 7.5 months with nivolumab vs 5.1 months with investigator's choice of chemotherapy (ICC). Estimated 6 month progression-free survival was 19.7% (nivolumab) vs 9.9% (ICC) [14]. In KEYNOTE-028, involving patients with unresectable or metastatic salivary gland carcinoma, the ORR was 12% after 20 months [15].

Despite the promise of PD-1/PD-L1 immunotherapy many patients do not respond and survival benefit is of the order of months. Alternative approaches targeting the PD-1 pathway are needed. There are no clinically available small molecule pharmacologic inhibitors of the PD-1/PD-L1 system. All available PD-1/PD-L1 strategies are antibodies requiring intravenous (i.v.) infusion and many experience grade $\geq 3$ immune-related adverse events. Immunotherapy has exorbitant cost and can have unpredictable and/or poor response in second-line treatment. Small-molecule inhibitors offer significant advantages such as favorable pharmacokinetics and druggability [16] and are often amenable to oral formulation. Patients on small molecule inhibitors can be dosed as outpatients. This means greater convenience, potential avoidance of i.v. administration and cost savings for chemotherapy units.

Here we demonstrate that systemically delivered flubendazole, available at low cost and without a prescription in Europe as an anthelmintic, is a novel small molecule pharmacologic inhibitor of PD-1. We performed studies in CB17/Icr-*Prkdcscid*/IcrIcoCrl SCID mice which lack T and B lymphocytes [17] since PD-1 expression is not confined to these cell types. Flubendazole abrogated melanoma growth and spread. It also suppressed angiogenesis and levels of myeloid-derived suppressor cells (MDSC), which typically inhibit the anti-tumor reactivity of immune cells and mediate resistance to immune checkpoint inhibitor (*i.e.* PD-1 antibody) therapy [18], but had no effect on PD-L1.

## 2. Materials and methods

*Tumor growth and metastasis.* Female 5 week old C.B.17 SCID mice (CB17/Icr-*Prkdcscid*/IcrIcoCrl) were sourced from Charles River Laboratories. Animals were inoculated subcutaneously with MDA-MB-435 cells ($2.5 \times 10^6$ cells/animal in 100 µl PBS) in the third mammary fat pad right flank region on Day 0. These cells were obtained from ATCC. Test articles were administered intraperitoneally (200 mg/kg, i.p.) or intratumorally (20 mg/kg, i.t.) once a day on a 5-days-on/2-days-off schedule. The compound was suspended at 9.6 mg/ml in vehicle (saline (0.9% NaCl) with 0.5% Tween 80 and 0.01% DMSO) and sonicated. Paclitaxel (15 mg/kg) was dosed i.v. twice a week. Animals were randomized Day 16 into groups of 10 with mean tumor volume ~83 $mm^3$ per group. Investigators were blinded to the nature of the test compounds except for paclitaxel. Animals were weighed twice per week. The general health condition and attitude of each animal was monitored daily throughout the study with detailed clinical observations performed twice per week. Tumors were measured by length and width in millimeters twice per week. Tumor volumes were calculated using formula V = L x W x W/2. If a second tumor occurred in a given animal, both tumor volumes were measured and their volumes were added together. After euthanasia by isoflurane overdose and cervical dislocation, the lungs of each animal were fixed in Bouin's solution. Metastatic nodules were counted and thoracic metastatic lesions were dissected and weighed. The protocol was approved by the Explora Biolabs' IACUC and ratified by the UNSW ACEC.

*Immunohistochemical staining of primary tumors and lung metastasis.* Rabbit monoclonal anti-CD31 (cat. ab182981), rabbit monoclonal anti-PD-1 (cat. ab214421), rabbit polyclonal anti-S100 (cat. ab868) and rabbit monoclonal anti-phospho-STAT3 ($Tyr^{705}$) (cat. ab76315) antibodies were obtained from Abcam. Rabbit polyclonal anti-PD-L1 (cat. PA5-20343) antibodies were obtained from ThermoFisher. Formalin-fixed or Bouin's solution-fixed, paraffin embedded sections were prepared from primary tumors or lungs. Heat-induced epitope retrieval was applied to all deparaffinized sections (4 µm Superfrost slides) with either citrate buffer, pH 6.0 (PD1, PD-L1, S100, p-STAT3 ($Tyr^{705}$)) or EDTA buffer, pH 9.0 (CD31) for 5 min at 110 °C. Sections were blocked with endogenous AP (Levamisole) blocking agent (DAKO, S2003) for 10 min and then with 2% skim milk for 20 min. Slides were incubated with primary antibody for 60 min at room temperature and then for 10 min with MACH3 Rabbit AP-Polymer Detection solution (probe incubation) (Biocare Medical, M3R533 G, H, L). After rinsing with buffer, the slides were incubated with MACH3 Rabbit AP-Polymer Detection solution (polymer incubation) (Biocare Medical, M3R533 G, H, L) for a further 10 min. Slides were incubated with red chromogen, (Warp Red™ Chromogen Kit) for 7 min and counterstained in haematoxylin and Scott blue. Slides were dried with filter paper and dehydrated in xylene then coverslipped.

Immunostained slides were scanned using an Aperio ScanScope XT slide scanner (Leica Biosystems, Mt Waverley, Vic, Australia) and images were captured using ImageScope software (Leica Biosystems). Integrated optical density (IOD) of positive staining (red chromogen) was assessed for CD31, PD1, PD-L1, S100 and p-STAT3 ($Tyr^{705}$) using Image-Pro Plus software (Cybernetics, Bethesda, MD, USA). Positive staining was the average of quantitation in 10-16 fields of view under 20× or 40× objective.

*Immunofluorescence staining of primary tumors.* Alexa Fluor® 594 anti-mouse/human CD11b (rat M1/70, cat. 101254) and Alexa Fluor® 488 anti-mouse Ly-6G/Ly-6C (Gr-1) (rat RB6-8C5, cat. 108417) were obtained from BioLegend. Formalin-fixed, paraffin embedded sections were prepared from primary tumors. Heat-induced epitope retrieval was applied to all deparaffinized sections (4 µm Superfrost slides) with citrate buffer, pH 6.0 for 5 min at 110 °C. Sections were blocked with 2% skim milk for 20 min. Slides were incubated with primary antibody for 120 min at room temperature. After rinsing with buffer, slides were incubated with 0.1% Sudan black (prepared with 70% Ethanol) for 1 min to block autofluorescence. Counterstained in ProLong™ Gold Antifade Mountant with DAPI (ThermoFisher cat. P36935) and then coverslipped. Fluorescence slides were scanned using an Aperio ScanScope FL slide scanner (Leica Biosystems, Mt Waverley, Vic, Australia) and images were captured using ImageScope software (Leica Biosystems). Integrated optical density (IOD) of positive staining (yellow) was assessed for $CD11b^+Gr1^+$ MDSC using Image-Pro Plus software (Cybernetics, Bethesda, MD, USA).

*Western blotting with MDA-MB-435.* MDA-MB-435 (ATCC) grown in 10% FBS/DMEM were seeded into 6 well plates ($1 \times 10^6$ cells/well). After 24 h, flubendazole (1 µM) or vehicle was added and after further 48 h, total cell lysates were prepared in RIPA buffer. Lysates (10 µg) were resolved by SDS-PAGE and Western blot analysis (in biological duplicates) was performed with rabbit monoclonal PD-1 antibodies (Abcam, cat. ab214421), mouse monoclonal anti-phospho-STAT3 ($Tyr^{705}$) (Cell Signaling, cat. 4113), rabbit monoclonal anti-STAT3 (Abcam, cat. ab109085) or mouse monoclonal β-actin antibodies (Sigma, cat. A5316), followed by horseradish peroxidase-conjugated secondary goat anti-rabbit (DAKO, cat. P0448) or goat anti-mouse (DAKO, cat. P0447) antibodies. Chemiluminescence was detected using the Western Lightning Chemiluminescence system (Thermo Scientific, USA) and ImageQuant™ LAS 4000 biomolecular imager (GE Healthcare Life Sciences, USA). Densitometry was performed using NIH Image J.

*Flow cytometry.* MDA-MB-435 cells were seeded into 6 well plates ($8 \times 10^5$ cells/well). After 24 h, flubendazole (1 µM) or vehicle was added and after further 48 h, the culture medium was removed and the cells were washed with PBS. Accutase was used to detach the cells. The

cells were washed and centrifuged at 300 g for 5 min, and resuspended at $5 \times 10^6$ cells/ml. One hundred μl was added to 12 × 75 mm tubes and BV421 conjugated mouse anti-human CD279 (PD-1) (BD, cat. 562516) or BV421 conjugated mouse $IgG_1$ (BD, cat. 562438) and incubated for 45 min at 22 °C, protected from light. Cells were washed twice with 1 ml of Stain Buffer, centrifuged and pellets were re-suspended in 0.5 ml Stain Buffer. Stained cell suspensions were analyzed by flow cytometry using a BD FACSCanto II.

*Statistical analysis.* Statistical analysis was performed as stated in the legends and significance indicated by asterisk(s). Standard inferential tests were used. If distribution was noted as not being normal, Mann Whitney (2 group comparisons) or Kruskal-Wallis (≥3 group comparisons) test was performed. Parametric data were analyzed by Student's *t*-test (2 group comparisons) or one-way ANOVA (≥3 group comparisons). Data was analyzed using GraphPad Prism 7 for MacOSX v7.0d. Data was considered significant when $P < 0.05$. *denotes $P < 0.05$, **denotes $P < 0.01$, ***denotes $P < 0.001$, ****denotes $P < 0.0001$.

## 3. Results

### 3.1. Flubendazole abolishes MDA-MB-435 melanoma growth

We determined whether flubendazole could influence the growth of solid tumors and spread in a mouse model using the aggressive triple negative (ERα, PR, HER2) human melanoma line, MDA-MB-435 [19,20], in a spontaneous metastasis model used for the preclinical evaluation of candidate anti-neoplastic therapies [21]. Flubendazole was administered i.p. or i.t. once a day on a 5-days-on/2-days-off schedule 16d after tumor cell inoculation for 4 weeks. Paclitaxel, dosed i.v. twice a week, was used as a positive control in the study. Flubendazole, dosed systemically, completely inhibited MDA-MB-435 tumor growth. Comparison of Day 49 primary tumor volumes with those of untreated Day 16 tumors revealed that tumors treated with flubendazole (i.p.) failed to grow (Fig. 1A, *upper*). There was no observable toxicity or weight loss in the tumor bearing mice (Fig. 1A, *lower*).

Further analysis revealed significant inhibition with flubendazole i.p. compared with vehicle within days of treatment (Fig. 1B). Flubendazole i.p. inhibition on Day 27 was more profound on Day 49 (Fig. 1B). Interestingly, there was no significant difference in tumor size between flubendazole i.p. and paclitaxel at either time (Fig. 1B). There was also no inhibition by flubendazole i.t. at either time (Fig. 1B). Tumors in mice treated with vehicle i.t. were larger than those in mice treated with vehicle i.p. at Day 27 (Fig. 1B) and Day 49 (Fig. 1B). This likely reflects altered tumor architecture when tumors are directly and repeatedly injected (5 consecutive days per week, i.t.) as recognized by others [22].

### 3.2. Flubendazole abolishes MDA-MB-435 metastasis

Flubendazole had dramatic effects on metastasis. Lung metastatic lesions visible in the vehicle group by Bouin's staining were virtually non-existent in flubendazole (i.p.)-treated mice as in paclitaxel-treated mice (Fig. 2A). Indeed, there was no difference in metastatic counts in lungs from mice treated with flubendazole or paclitaxel (Fig. 2B, *left*). Similarly, when metastatic lesions were excised and weighed, there was no difference between the flubendazole and paclitaxel groups (Fig. 2B, *right*). This indicates that the anti-metastatic efficacy of flubendazole was comparable to paclitaxel. Immunohistochemical staining for S100, a molecular marker for metastatic melanoma [23] revealed that flubendazole abolished metastatic spread to the lungs (Fig. 2C).

### 3.3. Flubendazole abrogates angiogenesis and phospho-STAT3 ($Tyr^{705}$) staining in MDA-MB-435 tumors

To determine the effect of flubendazole on tumor angiogenesis we performed immunohistochemical staining for the endothelial marker CD31/PECAM-1. Flubendazole almost completely suppressed CD31 expression indicating that flubendazole is a potent inhibitor of tumor angiogenesis (Fig. 3A). We also found that levels of active ($Tyr^{705}$) STAT3, transcription factor that regulates angiogenesis [24], were completely abrogated by flubendazole treatment (Fig. 3B).

### 3.4. Flubendazole inhibits PD-1 levels in MDA-MB-435 as tumors and in culture and abolishes $CD11b^+Gr1^+$ MDSC staining

Since systemic, but not local administration of flubendazole had profound effects on tumor growth and metastasis, we hypothesized that flubendazole might influence immune system through inhibiting negative immune system regulators such as PD-1 and/or PD-L1 and myeloid-derived suppressor cells (MDSC) within the tumors. MDSC can regulate tumor metastatic permissiveness in immunodeficient mice [25]. Immunohistochemical staining revealed that flubendazole completely abolished PD-1 levels in tumor tissue (Fig. 4A). In contrast, flubendazole had no effect on PD-L1 levels in the tumors (Fig. 4B).

We performed Western blot analysis to determine whether flubendazole is able to regulate PD-1 levels in the melanoma cells themselves. Indeed, flubendazole suppressed PD-1 expression in MDA-MB-435 cells (Fig. 4C, *left*). Flubendazole also inhibited STAT3 phosphorylation ($Tyr^{705}$) (Fig. 4C, *right*). PD-1 inhibition by flubendazole on MDA-MB-435 cells was further confirmed using flow cytometry (Fig. 4D).

That flubendazole can suppress tumor PD-1 levels led us to determine whether flubendazole also had effects on MDSCs. MDSCs inhibit innate and adaptive immunity [26] and facilitate tumor metastasis [25]. MDSCs also mediate resistance to immune checkpoint therapy [18]. STAT3 can regulate MDSC in other tumors such as head and neck cancer [27]. Immunohistochemical analysis revealed that flubendazole inhibited $CD11b^+Gr1^+$ MDSC [25] content within the tumors (Fig. 4E). Taken together, our findings show that flubendazole is a novel small molecule pharmacologic inhibitor of melanoma growth and spread, PD-1 and MDSC in tumor tissue.

## 4. Discussion

This present study demonstrates the anti-tumor and anti-metastatic activity of systemically delivered flubendazole in mice with no observable toxicity and that this involves profound inhibition of angiogenesis, PD-1 and MDSC but not PD-L1. PD-1 blockade is at the forefront of immunotherapy in a range of cancers. There are no clinically available small molecule inhibitors of PD-1 for any cancer. This report provides the first demonstration that flubendazole, a benzimidazole used for decades as an anthelmintic, serves as a small molecule inhibitor of PD-1 and MDSC.

Whilst others have reported the anti-tumor properties of flubendazole in various human cancers in immunocompetant and immunodeficient mice, such as triple negative breast cancer [28,29], leukemia [30], glioma [31] and myeloma [30], the effect of flubendazole on PD-1 or MDSC has not been investigated. These preclinical studies delivered flubendazole (10–50 mg/kg/day) i.p. daily or every two days for 16–25 days [28–31]. This demonstrates the capacity to use flubendazole systemically in a range of human cancer types. Since patient response to immune checkpoint inhibitor therapy does not appear to be restricted to a specific tumor type [10] the anti-cancer effects of flubendazole through PD-1 may not be restricted to melanoma. Flubendazole's inhibition of PD-1, and MDSC would have the effect of silencing their immunosuppressive effects [4,32] thereby preventing tumor growth and metastasis.

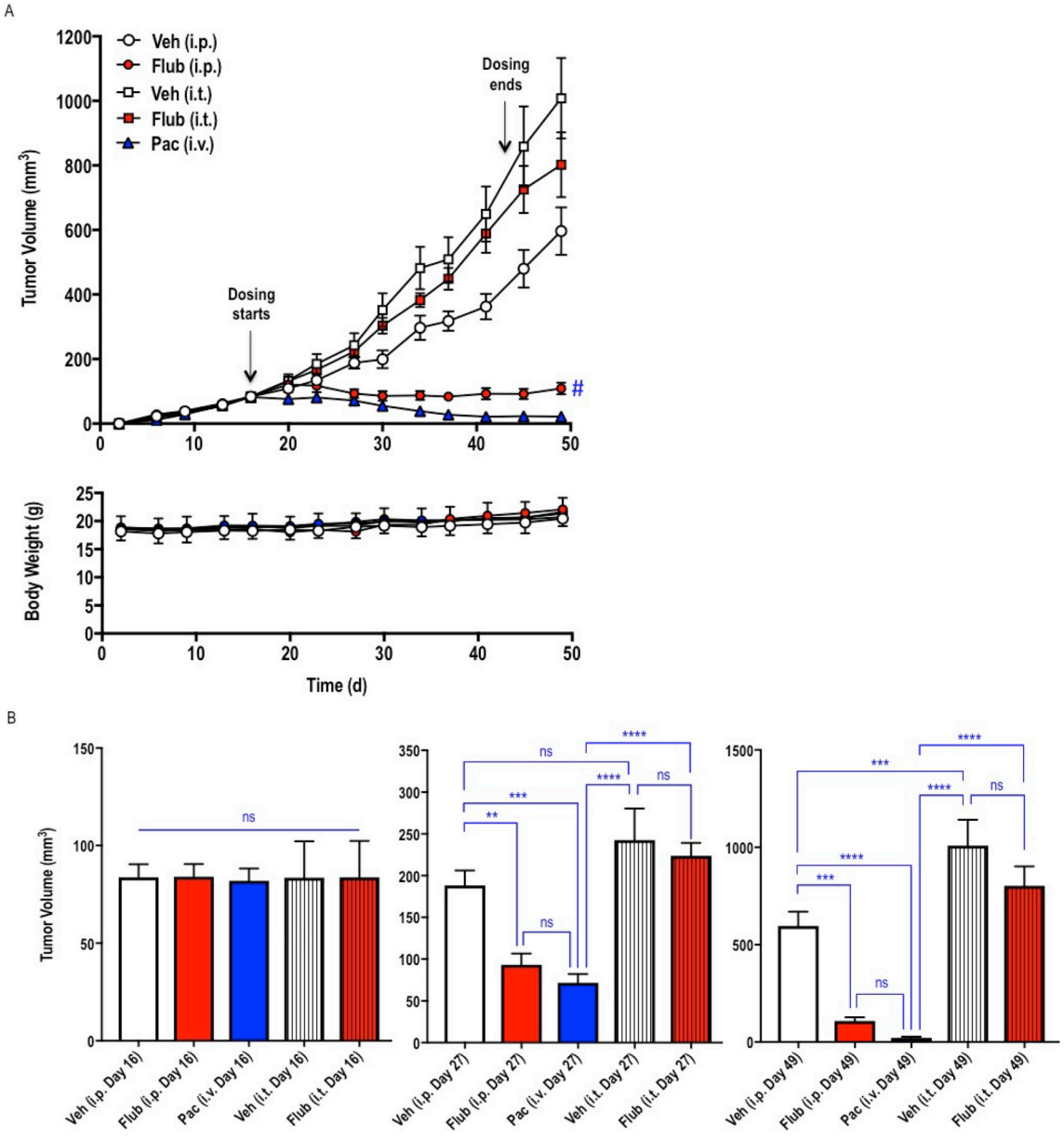


**Fig. 1. Flubendazole abolishes MDA-MB-435 melanoma growth. (A)** ***Upper,*** Female 5 week old C.B.17 SCID mice (CB17/Icr-*Prkdcscid*/IcrIcoCrl) were inoculated subcutaneously with MDA-MB-435 cells ($2.5 \times 10^6$ cells/animal) in the third mammary fat pad right flank region on Day 0. Flubendazole (Flub) or vehicle (Veh) was administered i.p. (200 mg/kg) or i.t. (20 mg/kg) once a day starting Day 16 on a 5-days-on/2-days-off schedule and stopping dosing on Day 43. Paclitaxel (Pac) was dosed i.v. (15 mg/kg) twice a week. # denotes no significant difference in tumor size between Day 16 and Day 49 in the flubendazole group (Student's *t*-test, n = 10 mice/group). ***Lower,*** Body weights of treated mice over the course of treatment. (**B**) Comparison of tumor volumes on Days 16, 27 and 49. Data was analyzed by one-way ANOVA (n = 10 mice/group).

Although flubendazole has been used extensively in humans and animals for > 3 decades and has a favorable safety profile, it has not been tested clinically for cancer. The drug appears to be well tolerated. No observable toxicity was reported in preclinical cancer models using flubendazole [28–31]. Its $LD_{50}$ in mice, rats and guinea pigs is > 5000 mg/kg [33,34]. Human subjects (neurocysticercosis) on 40 mg flubendazole/kg/day continuously for 10 days showed no toxicity, allergic reaction or adverse effect [35]. Similarly, alveolar echinococcosis patients on 50 mg flubendazole/kg/day for 16 months also showed no toxicity [36]. Flubendazole typically has low oral bioavailability. In humans, an oral dose of 100 or 2000 mg results in peak concentrations of 0.35 or 0.74 ng/ml within a few hours of administration. Bioavailability increases to 4.06 ng/ml after a 2000 mg dose if flubendazole is taken after a meal [34], which should be considered in any oral dosing regime involving patients. We are not aware of studies demonstrating the biodistribution of flubendazole in specific tissues or tumors when administered orally.

Selection of flubendazole dose in this study (200 mg/kg) was based in part on its high $LD_{50}$. We were also encouraged by flubendazole's comparative potency across a range of cancer cell types. While flubendazole has been tested in animal models of triple negative breast cancer [28,29], leukemia [30], glioma [31] and myeloma [30] at 10-50 mg/kg/day, recent comparative $IC_{50}$ analysis by Michaelis et al. [37] evaluating the effect of flubendazole on cancer cell viability across a large panel of cancer cell lines suggested that melanoma would require a higher dose of flubendazole than these other cancer types. We therefore used a higher dose of flubendazole to evaluate effects on melanoma growth and metastasis.

We show here that flubendazole inhibits active STAT3 ($Tyr^{705}$) levels in melanoma as solid tumors and cells. This, together with our

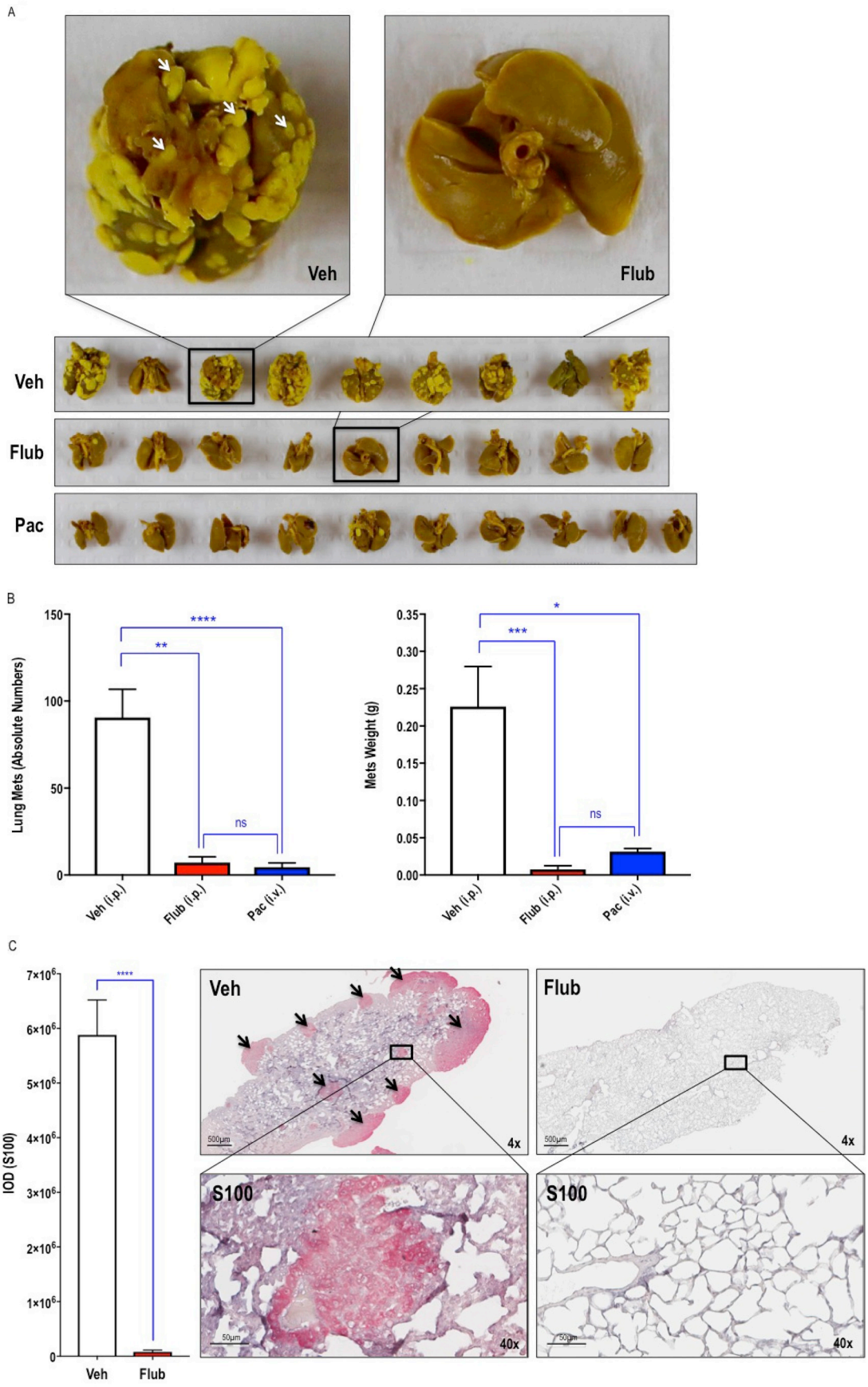


(caption on next page)

**Fig. 2. Flubendazole abolishes MDA-MB-435 metastasis.** **(A)** Lungs from vehicle, flubendazole (200 mg/kg i.p.) or paclitaxel (15 mg/kg i.v.) treated mice were fixed in Bouin's solution photographed. Metastatic lesions appear as yellow nodules. Arrows indicate representative nodules. **(B)** Metastatic nodules on Bouin's stained lungs were counted (***left***) or thoracic metastatic lesions dissected and weighed (***right***). Data was analyzed by Kruskal-Wallis test (n = 9–10 mice/group). **(C)** Immunohistochemical analysis was performed on lungs from flubendazole or vehicle-treated mice and antibodies to S100. Positive i.t. staining (red chromogen) was assessed using Image-Pro Plus® and expressed as integrated optical density (IOD, captures area and intensity) and the mean determined. Representative immunohistochemical staining is shown (***right***). Arrows indicate S100 staining. Data was analyzed by Mann Whitney test (n = 9 mice/group) (***left***). (For interpretation of the references to color in this figure legend, the reader is referred to the Web version of this article.)

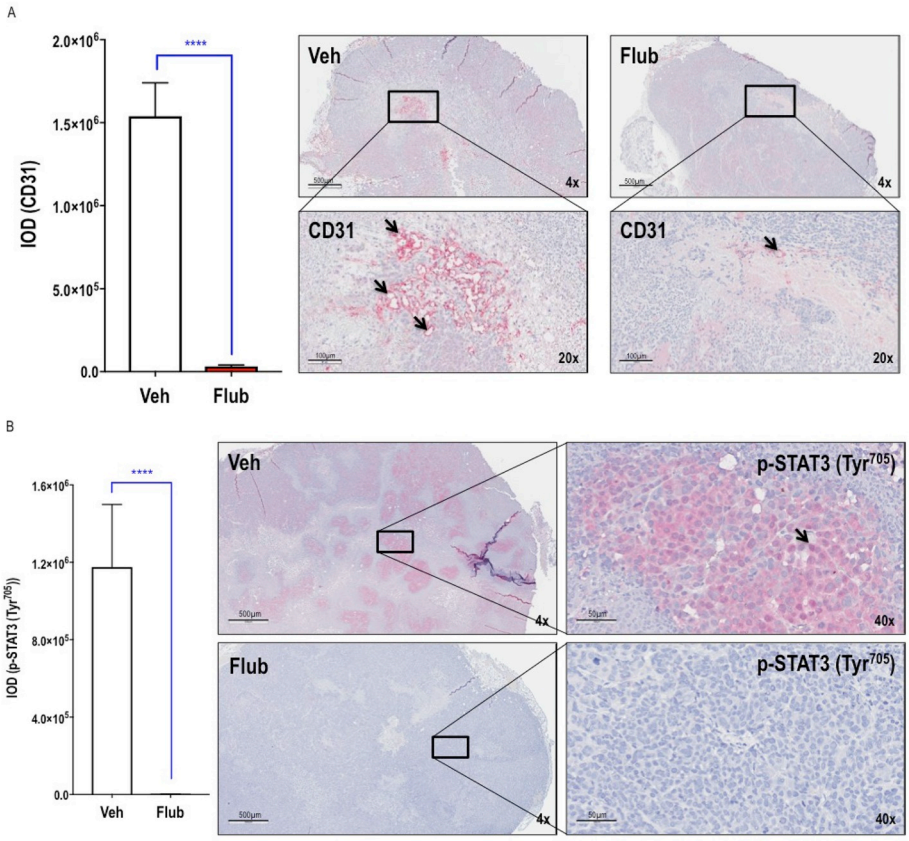


**Fig. 3. Flubendazole inhibits angiogenesis and p-STAT3 (Tyr$^{705}$) expression in MDA-MB-435 tumors.** Immunohistochemical analysis was performed on primary tumors from flubendazole or vehicle-treated mice with antibodies to (**A**) CD31 or (**B**) p-STAT3 (Tyr$^{705}$). IOD was assessed using Image-Pro Plus® and the mean determined. Representative immunohistochemical staining is shown (***right***). Arrows indicate positive staining. Data in (A) was analyzed by Student's *t*-test (n = 10 mice/group) or in (B) by Mann Whitney test (n = 9–10 mice/group) (***left***).

demonstration that flubendazole inhibits PD-1, is supported by previous reports showing that STAT3 regulates *pcdc1* transcription (*e.g.* Ref. [38]). Recent work has demonstrated that flubendazole can suppress p-STAT3 levels in breast cancer xenografts [28]. Notwithstanding this, flubendazole's effects may not be mediated through a single target. For example, flubendazole is also a known inhibitor of tubulin structure, polymerization and function [30]. In addition, flubendazole is one of a number of benzimidazole derivatives including, but not limited to, mebendazole, albendazole, oxibendazole and thiabendazole. Benzimidazoles are bicyclic aromatic organic compounds comprising a fused benzene and imidazole. The anti-cancer properties of several benzimidazole derivatives has been demonstrated including mebendazole for brain tumors [39], albendazole for colorectal cancer [40], oxibendazole for prostate cancer [41] and thiabendazole for malignant melanoma [42]. Although anthelmintics appear to act through tubulin, our findings suggest that the anticancer effects of these compounds may involve effects on PD-1, MDSC or STAT3. In other words, flubendazole's antitumor effects may not necessarily be mediated locally through tubulin [30]. A recent patent review identified a range of small molecule inhibitors of the PD-1/PD-L1 axis, largely through direct antagonism, but the general structures of these compounds lack the fused benzene and imidazole core of flubendazole [43] adding to our surprise that flubendazole can inhibit PD-1. STATs are activated (phosphorylated) by Janus kinase (JAK) [44]. The pharmacologic JAK inhibitor, JAK Inhibitor I (CAS 457081-03-7), which prevents STAT3 activation (Tyr$^{705}$) [45] also comprises a fused benzene and imidazole core.

This study used CB17/Icr-*Prkdcscid*/IcrIcoCrl SCID mice that possess a genetic autosomal recessive mutation designated Prkdc$^{scid}$ causing immunodeficiency affecting both T and B lymphocytes. Our understanding of PD-1's ability to guard against autoimmunity has typically focussed on T cells, by promoting apoptosis of antigen-specific T-cells and/or reducing apoptosis in regulatory T cells [46,47]. We chose to study flubendazole with MDA-MB-435 xenografts in SCID mice firstly, to demonstrate the ability of flubendazole to modulate PD-1 expression in a mouse model lacking T cells, and secondly, because there are no clinically available small molecule inhibitors of PD-1 for any cancer. By demonstrating that flubendazole inhibits tumor growth and spread in SCID mice (Figs. 1 and 2), and that this involves PD-1 inhibition (Fig. 4A), our study indicates that flubendazole can act independently of T cells. Our work also suggests that this small molecule has the potential to overcome current obstacles such as resistance to immune checkpoint inhibitor (*i.e.* PD-1 antibody) therapy. Such resistance may be mediated by aberrant processing or presentation of tumor antigens (*e.g.* impaired APC function and tumor MHC class I-deficiency) or severe T-cell exhaustion and immune suppressive cells (*e.g.* MDSCs) [18]. Further, PD-1 expression is not confined to T cells. PD-1 is also expressed on NK cells [48,49], tumor-associated macrophages [50], DCs [51] and cancer cells [7]. PD-1 is expressed on melanoma cells. Indeed, inhibition of melanoma PD-1 suppresses tumor growth independently of adaptive immunity [7]. This indicates that PD-1 blockade inhibiting

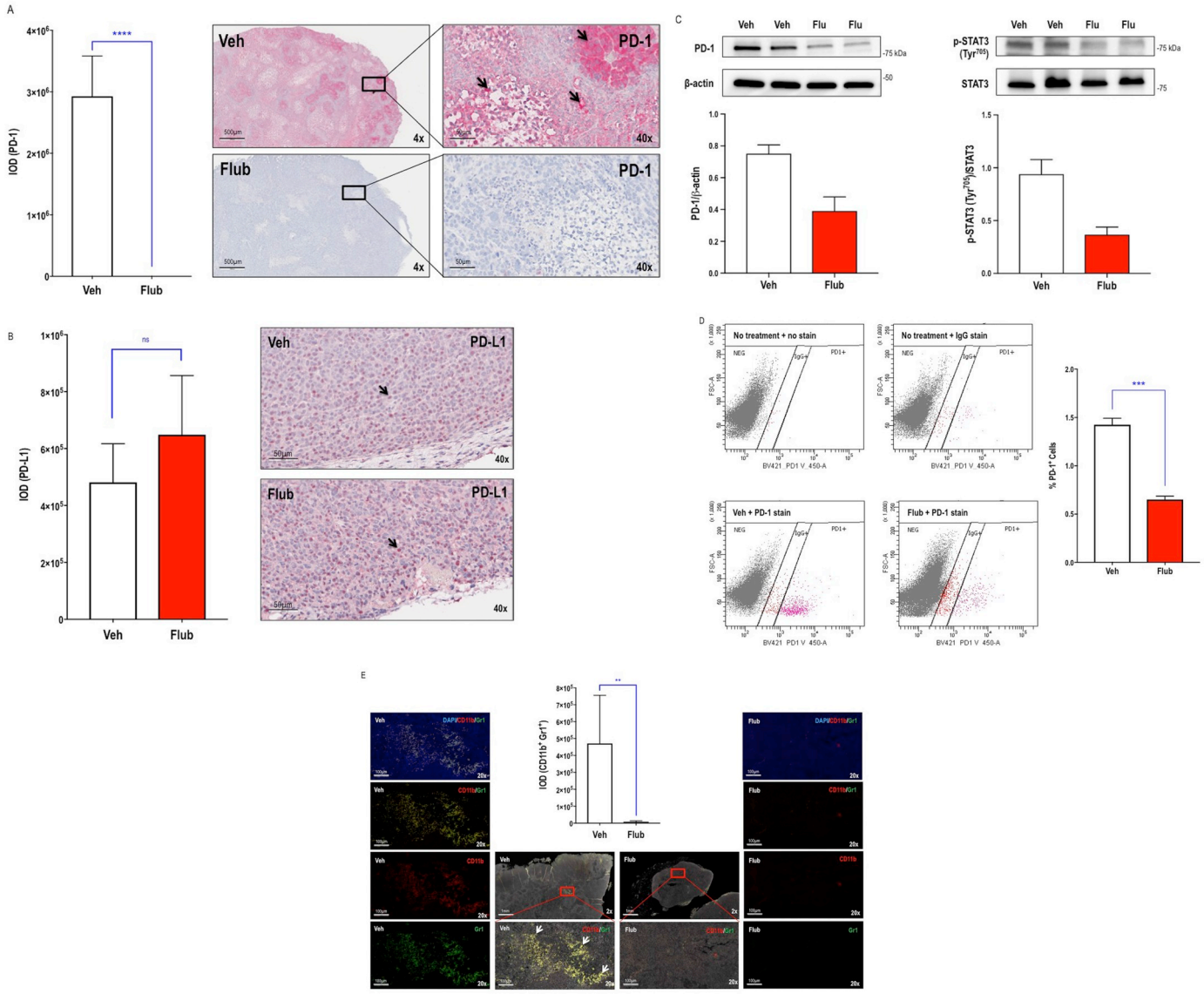


**Fig. 4. Flubendazole inhibits PD-1 and CD11b$^+$Gr1$^+$ MDSC levels in MDA-MB-435 tumors, and PD-1 and p-STAT3 (Tyr$^{705}$) in MDA-MB-435 cells.** Immunohistochemical analysis was performed on primary tumors from flubendazole or vehicle-treated mice with antibodies to (**A**) PD-1 or (**B**) PD-L1. IOD was assessed using Image-Pro Plus® and the mean determined. Representative immunohistochemical staining is shown (***right***). Arrows indicate positive staining. Data was analyzed by Mann Whitney test (n = 10 mice/group) (***left***). (**C**) Western blotting was performed with extracts of MDA-MB-435 (in biological duplicates) treated with flubendazole (1 μM) or vehicle. Membranes were treated with antibodies to PD-1, p-STAT3 (Tyr$^{705}$), total STAT3 or β-actin and then with horseradish peroxidase conjugated secondary goat anti-rabbit or goat anti-mouse antibodies. Approximate positions of molecular weight markers are shown. Data is representative of 2–3 independent experiments. Densitometry was performed using NIH Image J. (**D**) Flow cytometry was performed with MDA-MB-435 cells treated with flubendazole (1 μM) or vehicle for 48 h using a BD FACSCanto II. Data is representative of 4 independent experiments, each performed in biological duplicates. Data was analyzed by Student's *t*-test (n = 4) (***right***). (**E**) Immunohistochemical analysis was performed on tumors from flubendazole or vehicle-treated mice and antibodies to CD11b (red fluorescence) and Gr1 (green fluorescence). DAPI identifies nuclei. Slides were scanned using the AperioFL system and images were taken with identical settings and merged as indicated. Representative immunohistochemical CD11b$^+$Gr1$^+$staining is shown. Arrows indicate CD11b$^+$Gr1$^+$ staining. IOD was assessed using Image-Pro Plus® and the mean determined. Data was analyzed by Mann Whitney test (n = 10 mice/group). (For interpretation of the references to color in this figure legend, the reader is referred to the Web version of this article.)

tumor growth may be separate from its effects on the immune response. Moreover, high PD-1 expression has been reported on peripheral and tumor-infiltrating NK cells from tumor-bearing patients [52]. PD-1 expression on NK cells is associated with poor prognosis in some cancers [53]. Recent studies also indicate that PD-1 blockade on NK cells can enhance anti-tumor effects and regulate PD-1/PD-L1-based immunotherapy, especially for major histocompatibility complex (MHC) class I-deficient tumors that are poorly recognized by CD8$^+$ T cells and are associated with tumor progression [48,49]. That flubendazole inhibits PD-1 in a SCID mouse-based xenograft model indicates flubendazole's anti-tumor effects do not solely rely on T cells but instead, involves other immune cells and the tumor cells themselves. These mice reportedly have normal numbers and function of non-lymphoid blood cells, including NK cells, granulocytes and macrophages [17].

Paclitaxel was not used in this study to facilitate a mechanistic comparison with flubendazole. Different mechanisms are likely at play. In regard to tubulin, flubendazole inhibits tubulin polymerization by binding tubulin [30]. Paclitaxel, on the other hand, enhances the polymerization of tubulin and stabilizes against depolymerization [54]. Additionally, flubendazole was delivered i.t. and i.p., whereas paclitaxel was delivered i.v. The dose of paclitaxel (15 mg/kg) was vastly different from the efficacious dose of flubendazole (200 mg/kg i.p.).

When flubendazole was locally administered i.t. at a comparable dose to paclitaxel (20 mg/kg vs. 15 mg/kg, respectively), the former had no anti-tumor growth inhibitory or metastatic effect whereas the latter inhibited virtually completely. Moreover, flubendazole was delivered 5 times per week, whereas paclitaxel was delivered twice a week. There are also immune-related issues. Besides its tubulin polymerization properties, paclitaxel is now recognized as an immune response modulator involving T cells and other immune cell types. For example, Vicari et al. found that paclitaxel reduces regulatory T cells and inhibitory function and enhances anti-tumor effects in mice [55]. Machiels et al. showed that paclitaxel amplifies the T helper 1 neu-specific T-cell response [56]. Wanderley et al. reported paclitaxel reprograms M2-polarized macrophages (pro-tumor effect) to the M1-like phenotype (anti-tumor property) via the TLR4 receptor in breast and melanoma tumors [57]. Moreover, Shurin et al. and Zhong et al. showed paclitaxel up-regulates DC maturation and function [58], increases IL-12 expression [59], and changes the tumor microenvironment by altered the cytokine network at the tumor site [60].

The present study is the first to show that flubendazole blocks human melanoma growth and metastasis. This follows a recent report demonstrating that flubendazole induces mitotic catastrophe and apoptosis in melanoma cells (*i.e.* A-375, BOWES and RPMI-7951) [61]. We also show for the first time that flubendazole inhibits PD-1 and MDSC. This suggests that flubendazole blocks the permissive effect of PD-1/PD-L1 engagement on tumor growth whilst overcoming the immunosuppressive effects of MDSC.

## Conflicts of interest

The authors declare that they have no conflict of interest.

## Funding

This work was supported by grants from the National Health and Medical Research Council of Australia.

## Author contributions

LMK designed, directed and analyzed all aspects of this research; HX directed and analyzed the animal experiments; YL, GA, ME performed the work and analyzed the data.

## Acknowledgements

We thank Prof Larisa Haupt and KM Taufiqul Arif (Institute of Health and Biomedical Innovation, Queensland University of Technology) for MBA-MB-435 cells. We acknowledge the facilities, scientific and technical assistance of the National Imaging Facility at the Biological Resources Imaging Laboratory, Mark Wainwright Analytical Centre, UNSW) particularly Dr Fei Shang (Biomedical Imaging Facility) and Chris Brownlee (Flow Cytometry). We also thank Emeritus Prof Ian Dawes for critical review of the manuscript.

## Appendix A. Supplementary data

Supplementary data to this article can be found online at https://doi.org/10.1016/j.canlet.2019.05.026.

## References

[1] Z. Apalla, A. Lallas, E. Sotiriou, E. Lazaridou, D. Ioannides, Epidemiological trends in skin cancer, Dermatol. Pract. Concept. 7 (2017) 1–6.
[2] American_Cancer_Society, Treatment of Melanoma Skin Cancer, (2018) by Stage https://www.cancer.org/content/cancer/en/cancer/melanoma-skin-cancer/treating/by-stage/.
[3] J.J. Luke, K.T. Flaherty, A. Ribas, G.V. Long, Targeted agents and immunotherapies: optimizing outcomes in melanoma, Nat. Rev. Clin. Oncol. 14 (2017) 463–482.
[4] D.E. Dolan, S. Gupta, PD-1 pathway inhibitors: changing the landscape of cancer immunotherapy, Cancer Control 21 (2014) 231–237.
[5] A.H. Sharpe, K.E. Pauken, The diverse functions of the PD1 inhibitory pathway, Nat. Rev. Immunol. 18 (2018) 153–167.
[6] S. Du, N. McCall, K. Park, Q. Guan, P. Fontina, A. Ertel, T. Zhan, A.P. Dicker, B. Lu, Blockade of Tumor-Expressed PD-1 promotes lung cancer growth, OncoImmunology 7 (2018) e1408747.
[7] S. Kleffel, C. Posch, S.R. Barthel, H. Mueller, C. Schlapbach, E. Guenova, C.P. Elco, N. Lee, V.R. Juneja, Q. Zhan, C.G. Lian, R. Thomi, W. Hoetzenecker, A. Cozzio, R. Dummer, M.C. Mihm Jr., K.T. Flaherty, M.H. Frank, G.F. Murphy, A.H. Sharpe, T.S. Kupper, T. Schatton, Melanoma cell-intrinsic PD-1 receptor functions promote tumor growth, Cell 162 (2015) 1242–1256.
[8] S.N. Mueller, V.K. Vanguri, S.J. Ha, E.E. West, M.E. Keir, J.N. Glickman, A.H. Sharpe, R. Ahmed, PD-L1 has distinct functions in hematopoietic and non-hematopoietic cells in regulating T cell responses during chronic infection in mice, J. Clin. Invest. 120 (2010) 2508–2515.
[9] J. Gong, A. Chehrazi-Raffle, S. Reddi, R. Salgia, Development of PD-1 and PD-L1 inhibitors as a form of cancer immunotherapy: a comprehensive review of registration trials and future considerations, J. Immunother. Cancer 6 (2018) 8.
[10] K. Kataoka, S. Ogawa, Genetic biomarkers for PD-1/PD-L1 blockade therapy, Oncoscience 3 (2016) 311–312.
[11] J. Larkin, V. Chiarion-Sileni, R. Gonzalez, J.J. Grob, C.L. Cowey, C.D. Lao, D. Schadendorf, R. Dummer, M. Smylie, P. Rutkowski, P.F. Ferrucci, A. Hill, J. Wagstaff, M.S. Carlino, J.B. Haanen, M. Maio, I. Marquez-Rodas, G.A. McArthur, P.A. Ascierto, G.V. Long, M.K. Callahan, M.A. Postow, K. Grossmann, M. Sznol, B. Dreno, L. Bastholt, A. Yang, L.M. Rollin, C. Horak, F.S. Hodi, J.D. Wolchok, Combined nivolumab and ipilimumab or monotherapy in untreated melanoma, N. Engl. J. Med. 373 (2015) 23–34.
[12] R. Mehra, T.Y. Seiwert, S. Gupta, J. Weiss, I. Gluck, J.P. Eder, B. Burtness, M. Tahara, B. Keam, H. Kang, K. Muro, R. Geva, H.C. Chung, C.C. Lin, D. Aurora-Garg, A. Ray, K. Pathiraja, J. Cheng, L.Q.M. Chow, R. Haddad, Efficacy and safety of pembrolizumab in recurrent/metastatic head and neck squamous cell carcinoma: pooled analyses after long-term follow-up in KEYNOTE-012, Br. J. Cancer 119 (2018) 153–159.
[13] J. Bauml, T.Y. Seiwert, D.G. Pfister, F. Worden, S.V. Liu, J. Gilbert, N.F. Saba, J. Weiss, L. Wirth, A. Sukari, H. Kang, M.K. Gibson, E. Massarelli, S. Powell, A. Meister, X. Shu, J.D. Cheng, R. Haddad, Pembrolizumab for platinum- and cetuximab-refractory head and neck cancer: results from a single-arm, phase II study, J. Clin. Oncol. 35 (2017) 1542–1549.
[14] R.L. Ferris, G. Blumenschein Jr., J. Fayette, J. Guigay, A.D. Colevas, L. Licitra, K. Harrington, S. Kasper, E.E. Vokes, C. Even, F. Worden, N.F. Saba, L.C. Iglesias Docampo, R. Haddad, T. Rordorf, N. Kiyota, M. Tahara, M. Monga, M. Lynch, W.J. Geese, J. Kopit, J.W. Shaw, M.L. Gillison, Nivolumab for recurrent squamous-cell carcinoma of the head and neck, N. Engl. J. Med. 375 (2016) 1856–1867.
[15] R.B. Cohen, J.P. Delord, T. Doi, S.A. Piha-Paul, S.V. Liu, J. Gilbert, A.P. Algazi, S. Damian, R.L. Hong, C. Le Tourneau, D. Day, A. Varga, E. Elez, J. Wallmark, S. Saraf, P. Thanigaimani, J. Cheng, B. Keam, Pembrolizumab for the treatment of advanced salivary gland carcinoma: findings of the phase 1b KEYNOTE-028 study, Am. J. Clin. Oncol. 41 (2018) 1083–1088.
[16] K. Li, H. Tian, Development of small-molecule immune checkpoint inhibitors of PD-1/PD-L1 as a new therapeutic strategy for tumour immunotherapy, J. Drug Target. 27 (2019) 244–256.
[17] Charles_River, The CB17/Icr-Prkdcscid/IcrIcoCrl Mouse, (2009) https://www.criver.com/sites/default/files/resources/TheCB17Icr-PrkdcscidIcrIcoCrlMouseAFoxChaseSCID%C2%AESevereCombinedImmunodeficiencyModel.pdf.
[18] R.W. Jenkins, D.A. Barbie, K.T. Flaherty, Mechanisms of resistance to immune checkpoint inhibitors, Br. J. Cancer 118 (2018) 9–16.
[19] K.J. Chavez, S.V. Garimella, S. Lipkowitz, Triple negative breast cancer cell lines: one tool in the search for better treatment of triple negative breast cancer, Breast Dis. 32 (2010) 35–48.
[20] V.V. Prasad, R.O. Gopalan, Continued use of MDA-MB-435, a melanoma cell line, as a model for human breast cancer, even in year, 2014, NPJ Breast Cancer 1 (2015) 15002.
[21] C.M. Schmidt, S.L. Settle, J.L. Keene, W.F. Westlin, G.A. Nickols, D.W. Griggs, Characterization of spontaneous metastasis in an aggressive breast carcinoma model using flow cytometry, Clin. Exp. Metastasis 17 (1999) 537–544.
[22] J.L. Evelhoch, W. Negendank, F.A. Valeriote, L.H. Baker, Magnetic Resonance in Experimental and Clinical Oncology, Kluwer Academic, 1989.
[23] G. Henze, R. Dummer, H.I. Joller-Jemelka, R. Böni, B. G, Serum S100-a marker for disease monitoring in metastatic melanoma, Dermatology 194 (1997) 208–212.
[24] P. Gao, N. Niu, T. Wei, H. Tozawa, X. Chen, C. Zhang, J. Zhang, Y. Wada, C.M. Kapron, J. Liu, The roles of signal transducer and activator of transcription factor 3 in tumor angiogenesis, Oncotarget 8 (2017) 69139–69161.
[25] L.A. Mauti, M.A. Le Bitoux, K. Baumer, J.C. Stehle, D. Golshayan, P. Provero, I. Stamenkovic, Myeloid-derived suppressor cells are implicated in regulating permissiveness for tumor metastasis during mouse gestation, J. Clin. Invest. 121 (2011) 2794–2807.
[26] S. Ostrand-Rosenberg, P. Sinha, Myeloid-derived suppressor cells: linking inflammation and cancer, J. Immunol. 182 (2009) 4499–4506.
[27] J.F. Liu, W.W. Deng, L. Chen, Y.C. Li, L. Wu, S.R. Ma, W.F. Zhang, L.L. Bu, Z.J. Sun, Inhibition of JAK2/STAT3 reduces tumor-induced angiogenesis and myeloid-derived suppressor cells in head and neck cancer, Mol. Carcinog. 57 (2018) 429–439.
[28] E. Oh, Y.J. Kim, H. An, D. Sung, T.M. Cho, L. Farrand, S. Jang, J.H. Seo, J.Y. Kim, Flubendazole elicits anti-metastatic effects in triple-negative breast cancer via STAT3 inhibition, Int. J. Cancer 143 (2018) 1978–1993.

[29] Z.J. Hou, X. Luo, W. Zhang, F. Peng, B. Cui, S.J. Wu, F.M. Zheng, J. Xu, L.Z. Xu, Z.J. Long, X.T. Wang, G.H. Li, X.Y. Wan, Y.L. Yang, Q. Liu, Flubendazole, FDA-approved anthelmintic, targets breast cancer stem-like cells, Oncotarget 6 (2015) 6326–6340.
[30] P.A. Spagnuolo, J. Hu, R. Hurren, X. Wang, M. Gronda, M.A. Sukhai, A. Di Meo, J. Boss, I. Ashali, R. Beheshti Zavareh, N. Fine, C.D. Simpson, S. Sharmeen, R. Rottapel, A.D. Schimmer, The antihelmintic flubendazole inhibits microtubule function through a mechanism distinct from Vinca alkaloids and displays preclinical activity in leukemia and myeloma, Blood 115 (2010) 4824–4833.
[31] X. Zhou, J. Liu, J. Zhang, Y. Wei, H. Li, Flubendazole inhibits glioma proliferation by G2/M cell cycle arrest and pro-apoptosis, Cell Death Dis. 4 (2018) 18.
[32] V. Fleming, X. Hu, R. Weber, V. Nagibin, C. Groth, P. Altevogt, J. Utikal, V. Umansky, Targeting myeloid-derived suppressor cells to bypass tumor-induced immunosuppression, Front. Immunol. 9 (2018) 398.
[33] C. Mackenzie, A Review of Flubendazole and its Potential as a Macrofilariacide, Michigan State University, 2012.
[34] European_Medicines_Agency, FLUBENDAZOLE_EMEA/CVMP/33128/2006-FINAL, (2006).
[35] E. Tellez-Giron, M.C. Ramos, L. Dufour, M. Montante, E. Tellez Jr., J. Rodriguez, F. Gomez Mendez, E. Mireles, Treatment of neurocysticercosis with flubendazole, Am. J. Trop. Med. Hyg. 33 (1984) 627–631.
[36] A. Lassegue, J.M. Estavoyer, H. Minazzi, T. Barale, M. Gillet, D. Vuitton, J.P. Miguet, Treatment of human alveolar echinococcosis with flubendazole. Clinical, morphological and immunological study, Gastroenterol. Clin. Biol. 8 (1984) 314–320.
[37] M. Michaelis, B. Agha, F. Rothweiler, N. Loschmann, Y. Voges, M. Mittelbronn, T. Starzetz, P.N. Harter, B.A. Abhari, S. Fulda, F. Westermann, K. Riecken, S. Spek, K. Langer, M. Wiese, W.G. Dirks, R. Zehner, J. Cinatl, M.N. Wass, J. Cinatl Jr., Identification of flubendazole as potential anti-neuroblastoma compound in a large cell line screen, Sci. Rep. 5 (2015) 8202.
[38] J.W. Austin, P. Lu, P. Majumder, R. Ahmed, J.M. Boss, STAT3, STAT4, NFATc1, and CTCF regulate PD-1 through multiple novel regulatory regions in murine T cells, J. Immunol. 192 (2014) 4876–4886.
[39] M. De Witt, A. Gamble, D. Hanson, D. Markowitz, C. Powell, S. Al Dimassi, M. Atlas, J. Boockvar, R. Ruggieri, M. Symons, Repurposing mebendazole as a replacement for vincristine for the treatment of brain tumors, Molecular medicine (Cambridge, MA) 23 (2017) 50–56.
[40] A. Ehteda, P. Galettis, S.W.L. Chu, K. Pillai, D.L. Morris, Complexation of albendazole with hydroxypropyl-beta-cyclodextrin significantly improves its pharmacokinetic profile, cell cytotoxicity and antitumor efficacy in nude mice, Anticancer Res. 32 (2012) 3659–3666.
[41] Q. Chen, Y. Li, X. Zhou, R. Li, Oxibendazole inhibits prostate cancer cell growth, Oncol Lett 15 (2018) 2218–2226.
[42] J. Zhang, C. Zhao, Y. Gao, Y. Jiang, H. Liang, G. Zhao, Thiabendazole, a well-known antifungal drug, exhibits anti-metastatic melanoma B16F10 activity via inhibiting VEGF expression and inducing apoptosis, Pharmazie 68 (2013) 962–968.
[43] S. Shaabani, H.P.S. Huizinga, R. Butera, A. Kouchi, K. Guzik, K. Magiera-Mularz, T.A. Holak, A. Domling, A patent review on PD-1/PD-L1 antagonists: small molecules, peptides, and macrocycles (2015-2018), Expert Opin. Ther. Pat. 28 (2018) 665–678.
[44] C. Schindler, J.E. Darnell Jr., Transcriptional responses to polypeptide ligands: the JAK-STAT pathway, Annu. Rev. Biochem. 64 (1995) 621–651.
[45] S. Hashioka, A. Klegeris, H. Qing, P.L. McGeer, STAT3 inhibitors attenuate interferon-gamma-induced neurotoxicity and inflammatory molecule production by human astrocytes, Neurobiol. Dis. 41 (2011) 299–307.
[46] L.M. Francisco, P.T. Sage, A.H. Sharpe, The PD-1 pathway in tolerance and autoimmunity, Immunol. Rev. 236 (2010) 219–242.
[47] B.T. Fife, K.E. Pauken, The role of the PD-1 pathway in autoimmunity and peripheral tolerance, Ann. N. Y. Acad. Sci. 1217 (2011) 45–59.
[48] H. Seo, B.S. Kim, E.A. Bae, B.S. Min, Y.D. Han, S.J. Shin, C.Y. Kang, IL21 therapy combined with PD-1 and tim-3 blockade provides enhanced NK cell antitumor activity against MHC class I-deficient tumors, Cancer Immunol. Res. 6 (2018) 685–695.
[49] J. Hsu, J.J. Hodgins, M. Marathe, C.J. Nicolai, M.C. Bourgeois-Daigneault, T.N. Trevino, C.S. Azimi, A.K. Scheer, H.E. Randolph, T.W. Thompson, L. Zhang, A. Iannello, N. Mathur, K.E. Jardine, G.A. Kirn, J.C. Bell, M.W. McBurney, D.H. Raulet, M. Ardolino, Contribution of NK cells to immunotherapy mediated by PD-1/PD-L1 blockade, J. Clin. Invest. 128 (2018) 4654–4668.
[50] S.R. Gordon, R.L. Maute, B.W. Dulken, G. Hutter, B.M. George, M.N. McCracken, R. Gupta, J.M. Tsai, R. Sinha, D. Corey, A.M. Ring, A.J. Connolly, I.L. Weissman, PD-1 expression by tumour-associated macrophages inhibits phagocytosis and tumour immunity, Nature 545 (2017) 495–499.
[51] T.L. Sumpter, A.W. Thomson, The STATus of PD-L1 (B7-H1) on tolerogenic APCs, Eur. J. Immunol. 41 (2011) 286–290.
[52] D.M. Benson Jr., C.E. Bakan, A. Mishra, C.C. Hofmeister, Y. Efebera, B. Becknell, R.A. Baiocchi, J. Zhang, J. Yu, M.K. Smith, C.N. Greenfield, P. Porcu, S.M. Devine, R. Rotem-Yehudar, G. Lozanski, J.C. Byrd, M.A. Caligiuri, The PD-1/PD-L1 axis modulates the natural killer cell versus multiple myeloma effect: a therapeutic target for CT-011, a novel monoclonal anti-PD-1 antibody, Blood 116 (2010) 2286–2294.
[53] Y. Liu, Y. Cheng, Y. Xu, Z. Wang, X. Du, C. Li, J. Peng, L. Gao, X. Liang, C. Ma, Increased expression of programmed cell death protein 1 on NK cells inhibits NK-cell-mediated anti-tumor function and indicates poor prognosis in digestive cancers, Oncogene 36 (2017) 6143–6153.
[54] S.B. Horwitz, Taxol (paclitaxel): mechanisms of action, Ann. Oncol. 5 (Suppl 6) (1994) S3–S6.
[55] A.P. Vicari, R. Luu, N. Zhang, S. Patel, S.R. Makinen, D.C. Hanson, R.D. Weeratna, A.M. Krieg, Paclitaxel reduces regulatory T cell numbers and inhibitory function and enhances the anti-tumor effects of the TLR9 agonist PF-3512676 in the mouse, Cancer Immunol. Immunother. 58 (2009) 615–628.
[56] J.P. Machiels, R.T. Reilly, L.A. Emens, A.M. Ercolini, R.Y. Lei, D. Weintraub, F.I. Okoye, E.M. Jaffee, Cyclophosphamide, doxorubicin, and paclitaxel enhance the antitumor immune response of granulocyte/macrophage-colony stimulating factor-secreting whole-cell vaccines in HER-2/neu tolerized mice, Cancer Res. 61 (2001) 3689–3697.
[57] C.W. Wanderley, D.F. Colon, J.P.M. Luiz, F.F. Oliveira, P.R. Viacava, C.A. Leite, J.A. Pereira, C.M. Silva, C.R. Silva, R.L. Silva, C.A. Speck-Hernandez, J.M. Mota, J.C. Alves-Filho, R.C. Lima-Junior, T.M. Cunha, F.Q. Cunha, Paclitaxel reduces tumor growth by reprogramming tumor-associated macrophages to an M1 profile in a TLR4-dependent manner, Cancer Res. 78 (2018) 5891–5900.
[58] G.V. Shurin, I.L. Tourkova, M.R. Shurin, Low-dose chemotherapeutic agents regulate small Rho GTPase activity in dendritic cells, J. Immunother. 31 (2008) 491–499.
[59] G.V. Shurin, I.L. Tourkova, R. Kaneno, M.R. Shurin, Chemotherapeutic agents in noncytotoxic concentrations increase antigen presentation by dendritic cells via an IL-12-dependent mechanism, J. Immunol. 183 (2009) 137–144.
[60] H. Zhong, B. Han, I.L. Tourkova, A. Lokshin, A. Rosenbloom, M.R. Shurin, G.V. Shurin, Low-dose paclitaxel prior to intratumoral dendritic cell vaccine modulates intratumoral cytokine network and lung cancer growth, Clin. Cancer Res. 13 (2007) 5455–5462.
[61] K. Canova, L. Rozkydalova, D. Vokurkova, E. Rudolf, Flubendazole induces mitotic catastrophe and apoptosis in melanoma cells, Toxicol. In Vitro 46 (2018) 313–322.